ORIGINAL RESEARCH

Investigating the seismic performance of the honeycomb yielding damper (HYD)

Mortezaali Z.[1] , Peyman Shadman Heidari P.[2*], Ghanooni Bagha M.[3]

Abstract:

Today, the use of energy-dissipating system such as yielding metal damper in structures can improve the seismic performance of structures. One of the characteristics of metal yielding dampers is the ability to dissipate high energy and increase the ductility of the structural system, which can improve the ductility and energy absorption characteristics of the metal frame equipped with braces and prevent the brace from buckling during an earthquake. The purpose of this research is introduce a new form of yielding dampers called honeycomb yielding damper (HYD) with different dimensions and thickness along with evaluating and comparing the force-displacement diagrams and investigating the seismic parameters of this type of yielding damper. All modeling and validation of numerical samples were done by Ansys software. Non-linear analysis method is used in this research. The hysteresis curves are obtained under in-plane cyclic loads. The mechanical parameters such as ductility ratio, initial hardness, effective hardness and damping coefficient can be determin. The results of this research showed that the effective stiffness increases by increasing the length and thickness of the sample. The ductility ratio decreases by increasing the height of the sample. the effective stiffness decreases by increasing the height of the sample. The ductility ratio increases by increasing the height of the sample. Also, the effective damping coefficient decreases with the increase in the height of the samples, the effective damping coefficient increases with the increase in length and thickness of the samples.

Keywords:
Yielding honeycomb damper, Ductility ratio, Initial stiffness, Effective stiffness, Equivalent viscous damping.

✉*Corresponding author Email: peyman_shademan@yahoo.com, peyman.shademan@iau.ac.ir
1 Department of Civil Engineering, East Tehran Branch, Islamic Azad University, Tehran, Iran
2 Department of Civil Engineering, East Tehran Branch, Islamic Azad University, Tehran, Iran
3 Department of Civil Engineering, East Tehran Branch, Islamic Azad University, Tehran, Iran

1. Introduction

Earthquakes are the natural disasters that have occurred in recent years around the world, causing human and financial losses. damping systems are the most popular energy dissipation tools and are used in most projects. These instruments can a large amount of incoming earthquake energy with a predictable performance. In general, seismic control systems are divided into two categories, active control and passive control. Therefore, the use of passive control seismic design methods, such as yielding metal dampers that have the ability to dissipate the incoming energy of earthquake to structures, can improve the seismic performance of structures. The performance of metal dampers based on their non-linear behavior is one of the most effective mechanisms of damping and absorption of energy input to the structure during an earthquake. Kelly et al [1] used the idea of metallic dampers to absorb earthquakes energy in the structure. They introduced several hysteretic energy absorption mechanisms in structures. Skinner et al [2, 3] proposed several yielding metal dampers, including torsion beam dampers, bending beam dampers, and U-shaped dampers. Kasai and Popov [4] presented yielding damper using steel plate and stiffener. They tested it and introduced the hysteresis curve. Bergman and Goel [5] proposed flexural yielding metallic dampers. They tested added damping and stiffness (ADAS) and Triangular-ADAS (TADAS) systems. In ADAS and TADAS dampers are used parallel X and V shaped steel plates, respectively. Whittaker et al [6] tested X-shaped metallic dampers as ADAS under cyclic load. Tsai et al [7], in order to fix the defects of the XADAS dampers, studied TADAS triangular steel plate dampers. Also, they developed a simple mathematical model for force-displacement, which was reasonably accurate compared to laboratory work. Dargush and Soong [8] conducted a more detailed study of the phenomenon of fatigue in low cycles based on the behavioral theories of TADAS dampers and developed their analytical models. Gang Li and Hongnan Li [9] presented a new idea for designing metallic damper. They tested dual functions metallic damper (DFMD) with quasi-static loading. Soni and Sanghvi [10] described a technique to find out combined stiffness of model equipped with ADAS damper. They proposed a mathematical model. Teruna et al [11] investigated four steel damper specimens with specific geometry. They obtained energy absorption capabilities, hysteresis loop and stiffness in specimens. Sahoo et al [12] investigated passive energy dissipation of steel plates in both flexure and shear yielding under cyclic loading. Their specimens consist of two flexure (end) plates of X-shape and a shear (web) plate of rectangular shape. Garivani et al [13] introduced a new type of flexural yielding metallic damper and they called comb-teeth damper (CTD). Their damper included number of teeth steel plates that absorb energy through in-plane flexural yielding. Ghaedi et al [14] introduced a new hysteretic metallic bar damper that they named bar damper (BD). BD included three simple steel plates and a number of solid bars which dissipate input energy due to vibration loads through flexural yielding. Kiani [15] designed a model of yielding damper with the hip, chevron, gate, diagonal and knee braces, whose performance reduced the base shear of the system. Moghadisi and Namazi [16] regarding the design of three earthquake-resistant systems, including a structure with a damper, a structure without a damper, and a structure with a chevron brace, which showed that the base shear in a structure with a yield damper is reduced compared to other structures. They also showed that the performance of the structure with yielding damper is better during earthquakes. Yang et al [17] investigated the experimental results of the new HSF honeycomb structure, which shows that the use of the proposed HSF honeycomb structure can provide stable energy dissipation capability as an efficient metal damper for earthquake parameters. Yang et al [18] in a detailed experimental study on the new metal WWFF damper in order to investigate the effect of design

parameters such as aspect ratio and slenderness on structural response such as yield strength and stiffness showed that this damper has a stable energy dissipation capacity and can It can be used as an efficient and strong metal damper. Peyman Shadman Heidari [19] presented a new type of metal shear yielding damper in which a perforated shear plate is used and by changing the location and diameter of the holes in DPMD dampers, he investigated the mechanical characteristics of different samples of DPMD dampers.

The purpose of this research is introduce the new form of yielding dampers with different geometry under the name of honeycomb yielding dampers (HYD) with different dimensions and thicknesses. In this research determines their mechanical and seismic characteristics of samples were investigated with the hysteresis curves of the honeycomb yielding damper samples under in-plane cyclic load can determined mechanical parameters such as ductility ratio, initial stiffness, effective stiffness, total dissipated energy, dissipated energy in the last cycle, elastic strain energy, equivalent viscous damping (EVD) and equivalent plastic strain (EPS).

2. Honeycomb yielding damper (HYD)

2.1. Geometry of Honeycomb damper

ADAS dampers are usually used in steel bracing frames, as shown in Figure 1. The HYD dampers can create by drilling a hexagonal shape on a metal sheet and use in metal frame with a chevron brace as shown in Figure 1 and 2. In this research, 28 numerical models are proposed based on different thickness, length and height. The thickness of all samples was considered as 0.48, 0.72, 0.96 and 1.44 cm, respectively. The lengths of all samples are 41.80, 52.96, 64.12 and 75.28 cm, respectively. Also, samples were considered with different heights of 20.32, 26.76, 33.20 and 39.65 cm. The length of each side of the hexagon is 3.72 cm and the angle between the sides is 120 degrees. Figure 3 shows the modeling of the honeycomb damper with different lengths, heights and thicknesses. Table 1 shows the specifications and dimensions of the HYD dampers. The Table 1 shows specifications and different dimensions of HYD dampers.

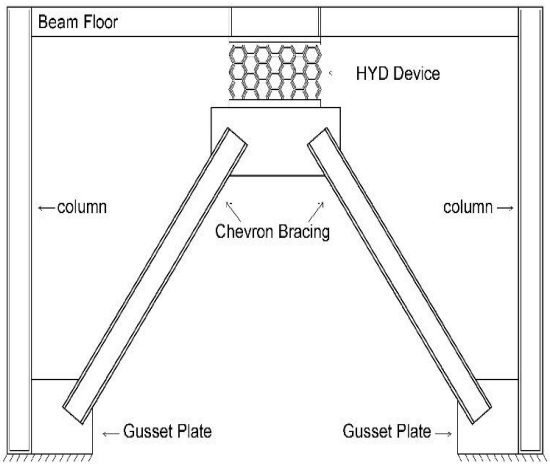

Fig. 1. Frame system and HYD position

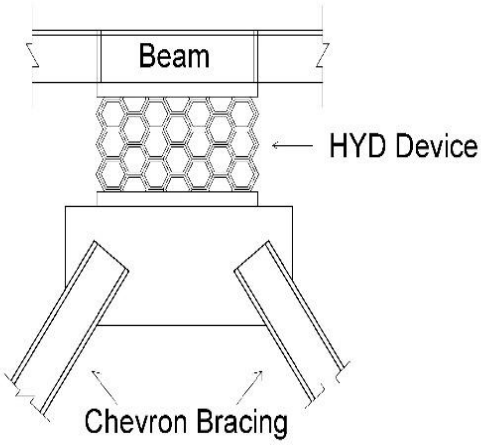

Fig. 2. Connection of HYD to beam and bracing

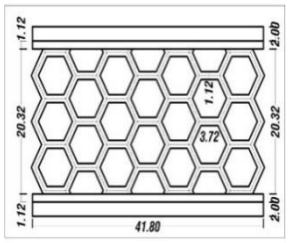

HYD-1-1-1-1

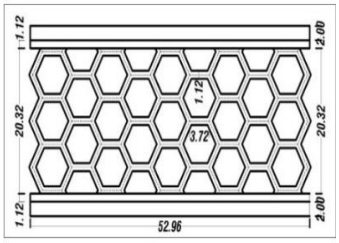

HYD-1-2-1-1

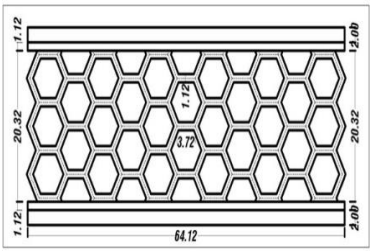

HYD-1-3-1-1

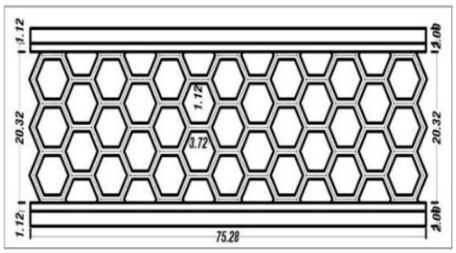

HYD-1-4-1-1

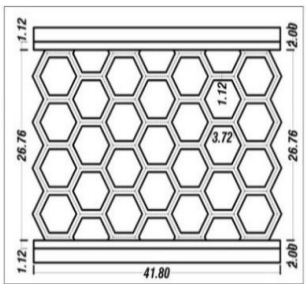

HYD-1-1-2-1

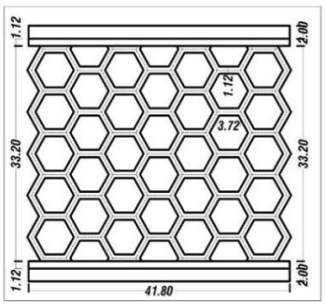

HYD-1-1-3-1

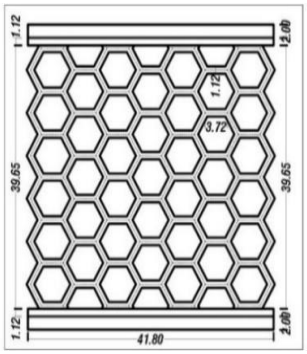

HYD-1-1-4-1

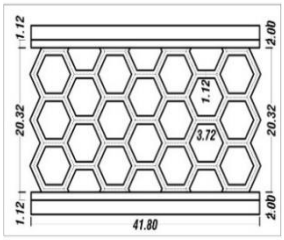

HYD-2-1-1-1

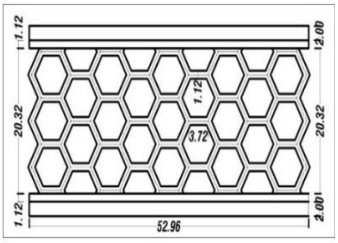

HYD-2-2-1-1

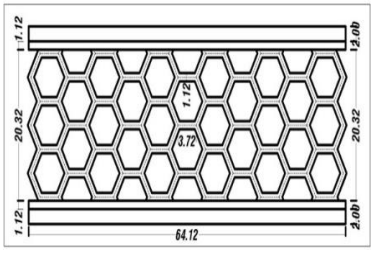

HYD-2-3-1-1

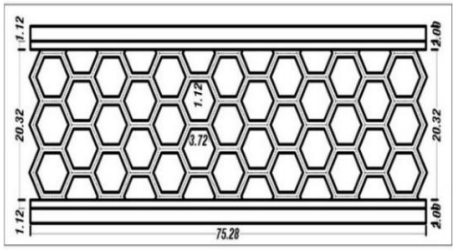

HYD-2-4-1-1

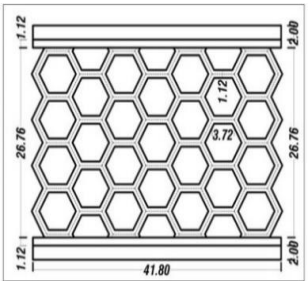

HYD-2-1-2-1

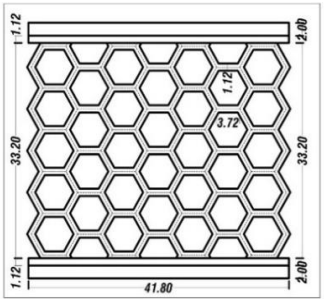

HYD-2-1-3-1

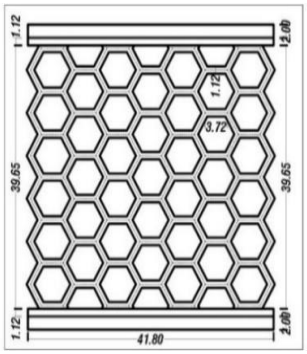

HYD-2-1-4-1

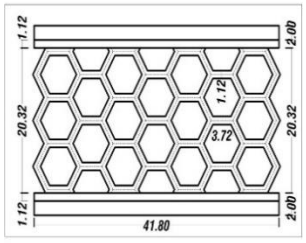

HYD-3-1-1-1

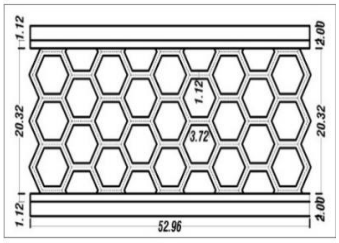

HYD-3-2-1-1

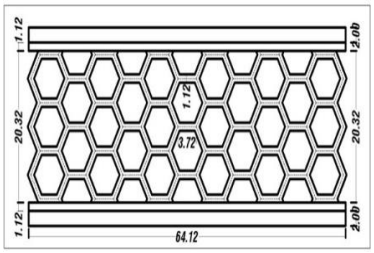

HYD-3-3-1-1

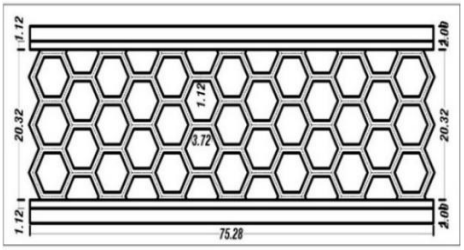

HYD-3-4-1-1

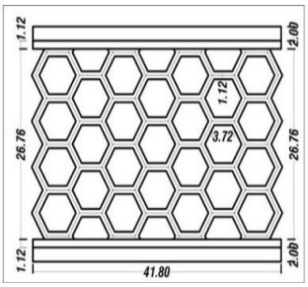

HYD-3-1-2-1

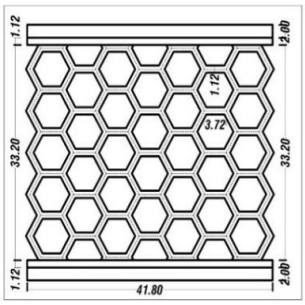

HYD-3-1-3-1

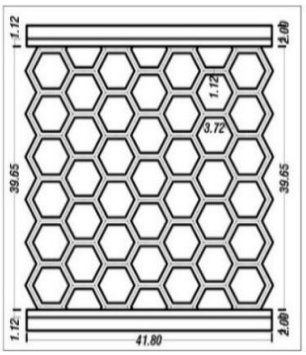

HYD-3-1-4-1

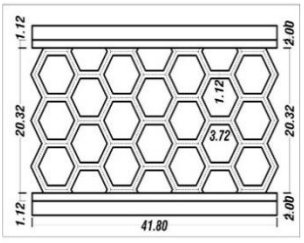

HYD-4-1-1-1

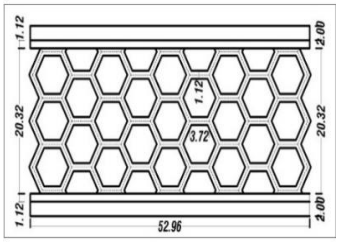

HYD-4-2-1-1

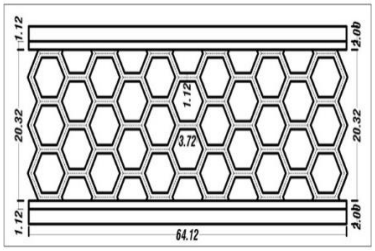

HYD-4-3-1-1

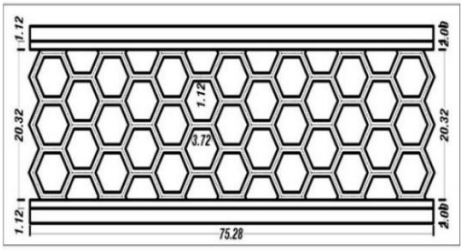

HYD-4-4-1-1

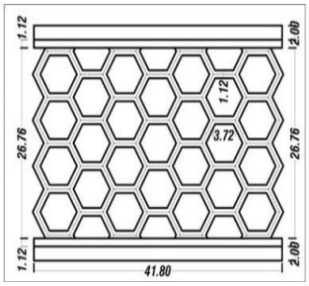

HYD-4-1-2-1

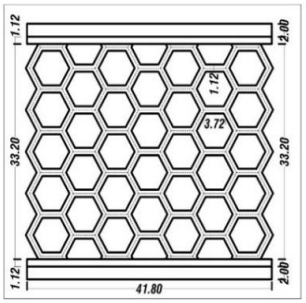

HYD-4-1-3-1

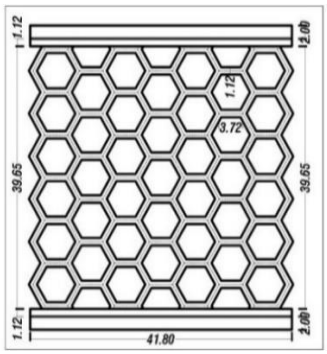

HYD-4-1-4-1

Fig.3. HYD damper modeling with different lengths, heights and thicknesses.

Table 1. Specifications and different dimensions of HYD dampers

Number	Sample	thickness t_p (cm)	Length L(cm)	Hight H(cm)	Length of the hexagon h(cm)
1	HYD-1-1-1-1	0.48	41.80	20.32	3.72
2	HYD-1-2-1-1	0.48	52.96	20.32	3.72
3	HYD-1-3-1-1	0.48	64.12	20.32	3.72
4	HYD-1-4-1-1	0.48	75.28	20.32	3.72
5	HYD-1-1-2-1	0.48	41.80	26.76	3.72
6	HYD-1-1-3-1	0.48	41.80	33.20	3.72
7	HYD-1-1-4-1	0.48	41.80	39.65	3.72
8	HYD-2-1-1-1	0.72	41.80	20.32	3.72
9	HYD-2-2-1-1	0.72	52.96	20.32	3.72
10	HYD-2-3-1-1	0.72	64.12	20.32	3.72
11	HYD-2-4-1-1	0.72	75.28	20.32	3.72
12	HYD-2-1-2-1	0.72	41.80	26.76	3.72
13	HYD-2-1-3-1	0.72	41.80	33.20	3.72
14	HYD-2-1-4-1	0.72	41.80	39.65	3.72
15	HYD-3-1-1-1	0.96	41.80	20.32	3.72
16	HYD-3-2-1-1	0.96	52.96	20.32	3.72
17	HYD-3-3-1-1	0.96	64.12	20.32	3.72
18	HYD-3-4-1-1	0.96	75.28	20.32	3.72
19	HYD-3-1-2-1	0.96	41.80	26.76	3.72
20	HYD-3-1-3-1	0.96	41.80	33.20	3.72
21	HYD-3-1-4-1	0.96	41.80	39.65	3.72
22	HYD-4-1-1-1	1.44	41.80	20.32	3.72
23	HYD-4-2-1-1	1.44	52.96	20.32	3.72
24	HYD-4-3-1-1	1.44	64.12	20.32	3.72
25	HYD-4-4-1-1	1.44	75.28	20.32	3.72
26	HYD-4-1-2-1	1.44	41.80	26.76	3.72
27	HYD-4-1-3-1	1.44	41.80	33.20	3.72
28	HYD-4-1-4-1	1.44	41.80	39.65	3.72

2.2. Loading pattern and material properties

In order to evaluate the performance of honeycomb yielding dampers was used AISC 341-16[20] cyclic loading pattern. The relative deformation between the upper and lower plates of the damper is equal to 0.00375 radians for steps 1 to 12 in 6 cycles. for steps 13 to 24 for 6 cycles, the relative deformation between the upper and lower plates of the damper is equal to 0.005 radians for steps 25 to 36 in 6 cycles, the relative deformation is equal to 0.0075 radians for steps 37 to 44 in 4 cycles, the relative deformation is equal to 0.01 radians for steps 45 to 48 in 2 cycles, the relative deformation between the upper and lower plates of the damper is equal to 0.015 radians for steps 49 to 52 in 2 cycles, the relative deformation is equal to 0.02 radians for steps 53 to 56 in 2 cycles, the relative deformation between the upper and lower plates of the damper is equal to 0.03 radians for steps 57 to 60 in 2 cycles, the relative deformation between the upper and lower plates of the damper is equal to 0.04 radians and for steps 61 to 100 in 2 cycles, the relative deformation between the upper and lower plates of the damper is equal to 0.01 radians according to Figure 4. In this research, materials with the characteristics of the stress-strain curve used according to Figure 5

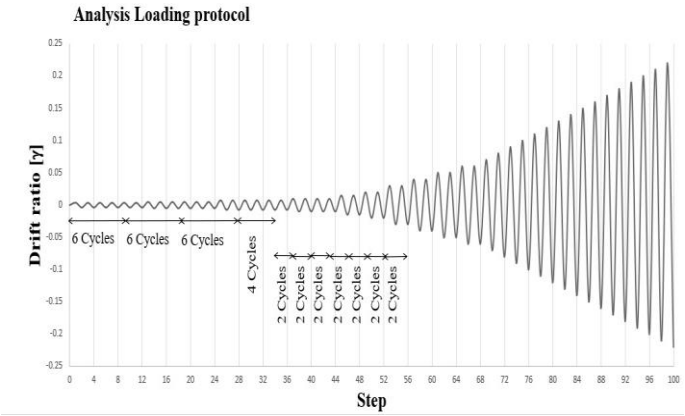

Fig. 4. AISC 341-16[20] cyclic loading pattern

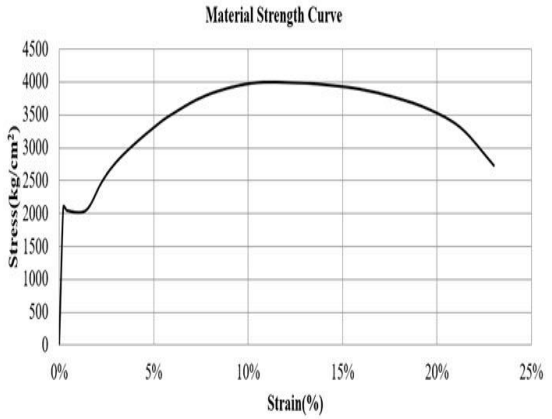

Fig. 5. Stress-strain curve

3. Finite Element Modeling procedure

3.1. FEMs of HYD

To study the mechanical parameters of the honeycomb metallic damper used nonlinear finite element (FE) analyses with ANSYS R16 FEM [21] software. The 28 finite element models were modeled with different thickness, length and height. Steel plate elements were modeled using a 3D solid element. SOLID 185 (brick 8 node 185) element was used for modeling of proposed samples.

Multilinear kinematic hardening plastic model [21] was used to model the plasticity and cyclic inelastic behavior of steel material, respectively. The transitional degree of freedom in the Z and Y directions are closed in order to prevent out of plane buckling of the end plate. Mesh sensitivity analysis was performed to find proper element sizes in the FEMs. Figure 6 shows the FEMs of the HYD-1-1-1-1, HYD-1-2-1-1, HYD-1-3-1-1, HYD-1-4-1-1, HYD-1-1-2-1, HYD-1-1-3-1 and HYD-1-1-4-1.

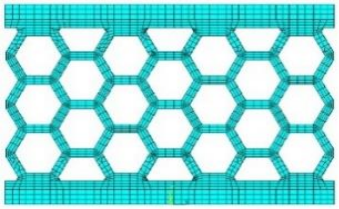

HYD-1-1-1-1

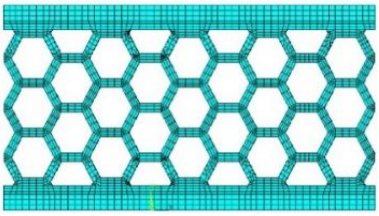

HYD-1-2-1-1

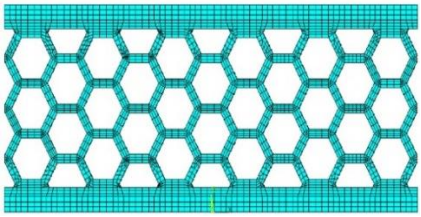

HYD-1-3-1-1

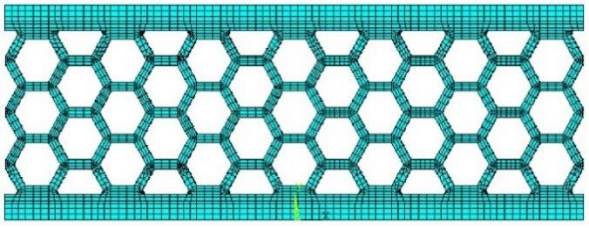

HYD-1-4-1-1

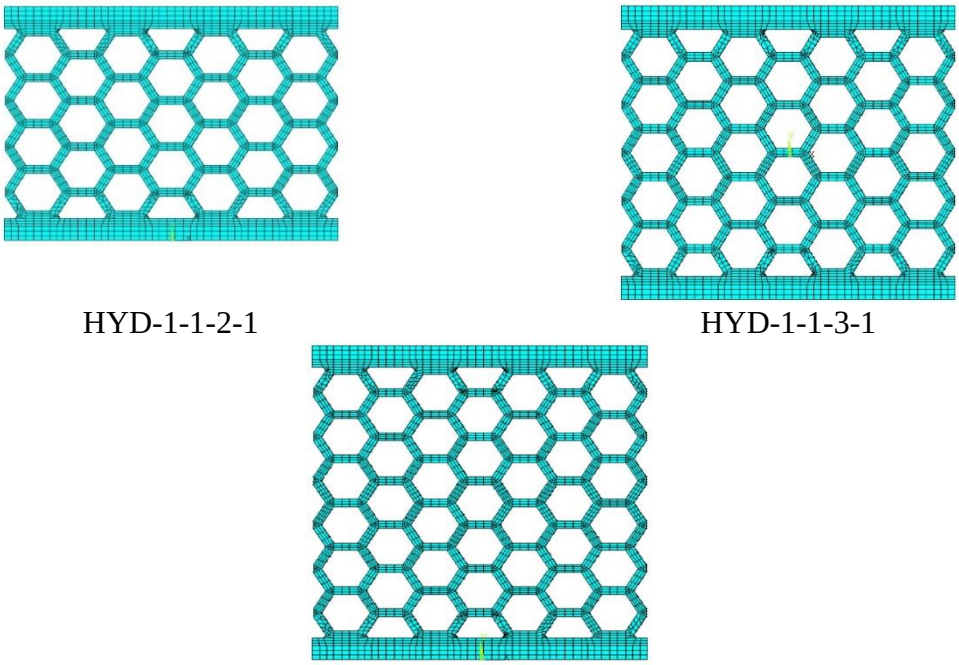

Fig. 6. Finite element models of HYD sample

3.2. FEM of HSF experimental specimen

The experimental specimen (HSF [17]) was modeled in ANSYS R16 FEM [21] software in order to validate the FEMs. The displacement ratio applied in the upper sample is γ=10%. The details of the experimental specimen and finite element modeling with ANSYS R16 FEM software [21] show in the Figures 7 and 8 respectively.

The results of analytical analysis were compared experimental results. There is an acceptable agreement between the results of analytical and experimental studies according to Figure 9 and 10. Figure 11 shows the comparison between the hysteresis curves of the HSF experimental specimen [17] and the FEM hysteresis curves.

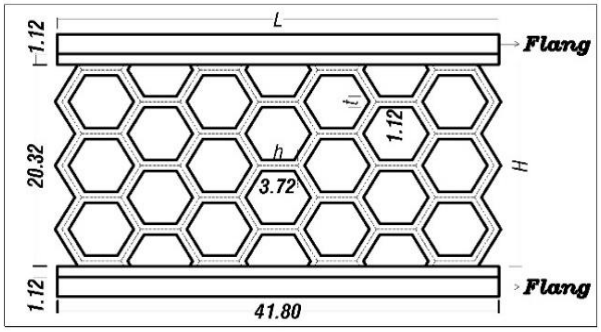

Fig. 7. Details of HSF experimental specimen [17]

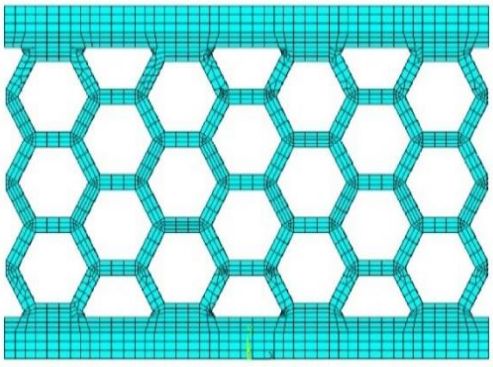

Fig. 8. Finite element modeling of HSF experimental sample [17]

Fig. 9. Deformation after loading in HSF experimental specimen [17]

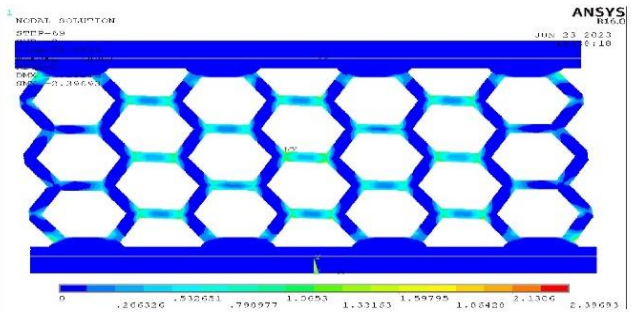

Fig. 10. Deformation after applying loading in the FEM sample with ANSYS R16 FEM[21]

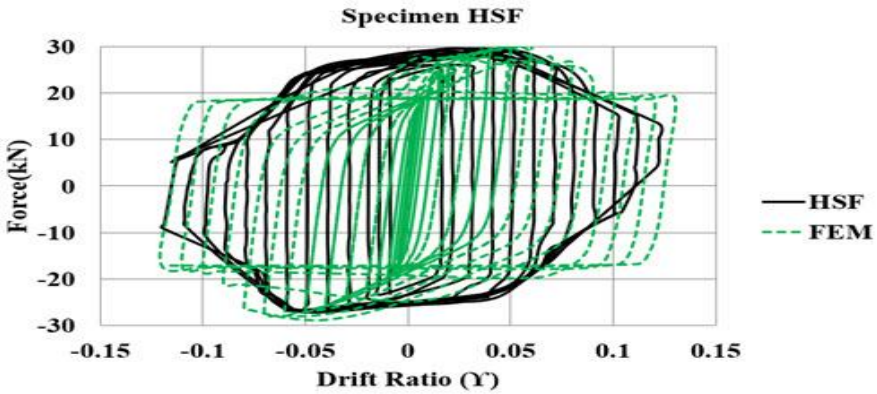

Fig. 11. Comparison between the hysteresis curve of the HSF experimental specimen [17] and the FEM sample with ANSYS R16 FEM software [21]

3.3. Hysteresis behavior of HYDs

Hysteresis curves used to determine the mechanical parameters of the HYD proposed damper. In the force-displacement hysteresis Curve can be obtained parameters such as yield force, Yield displacement, ultimate force, and ultimate displacement. For this purpose, force-displacement hysteresis curves of analytical samples were determined. Figure 12 shows the force-displacement hysteresis curves of the HYD dampers.

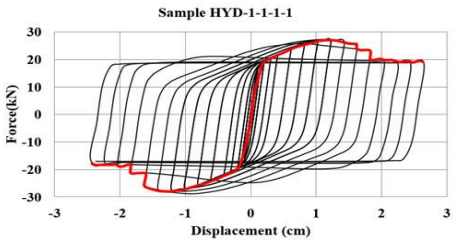

HYD-1-1-1-1

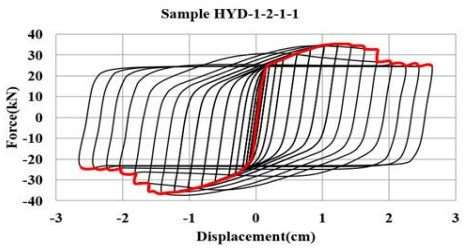

HYD-1-2-1-1

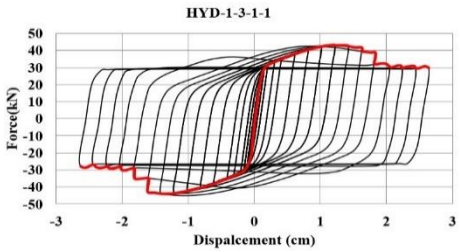

HYD-1-3-1-1

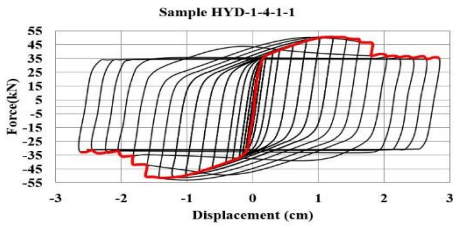

HYD-1-4-1-1

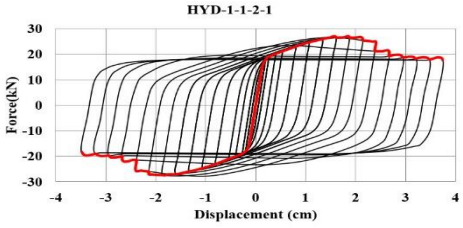

HYD-1-1-2-1

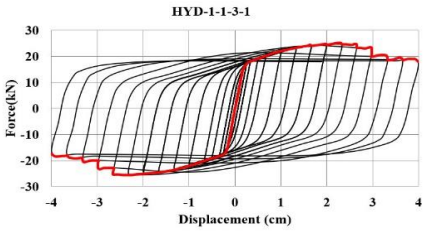

HYD-1-1-3-1

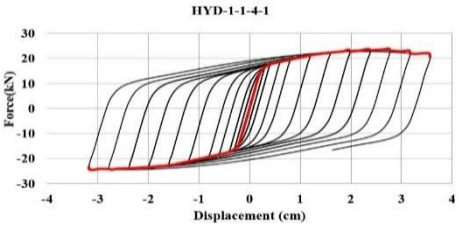

HYD-1-1-4-1

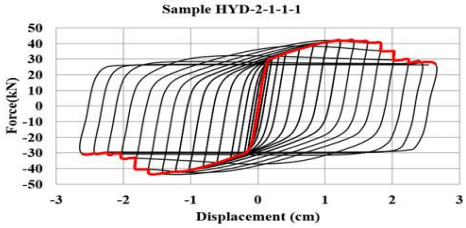

HYD-2-1-1-1

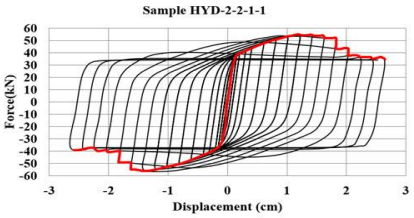

HYD-2-2-1-1

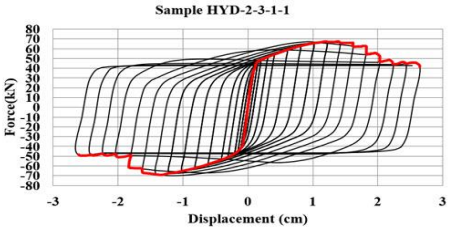

HYD-2-3-1-1

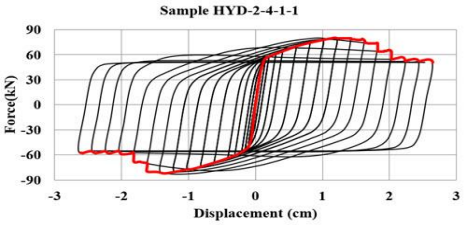

HYD-2-4-1-1

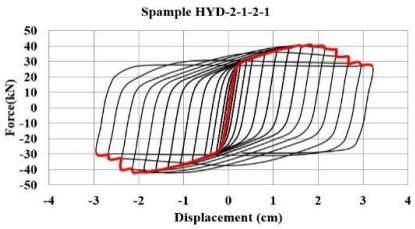

HYD-2-1-2-1

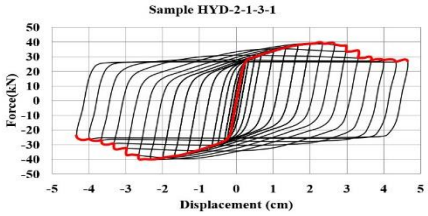

HYD-2-1-3-1

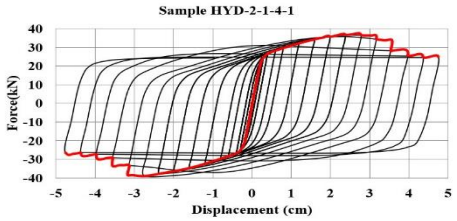

HYD-2-1-4-1

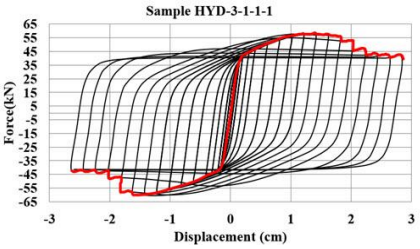

HYD-3-1-1-1

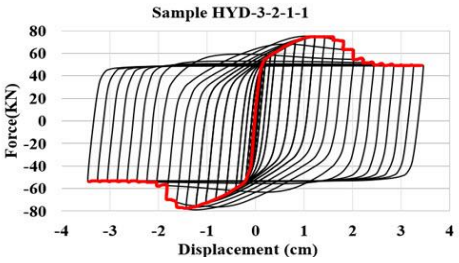

HYD-3-2-1-1

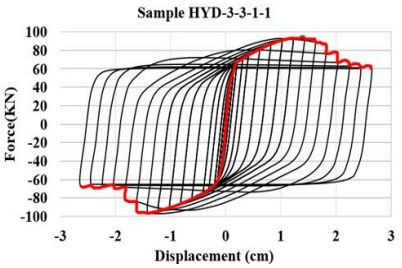

HYD-3-3-1-1

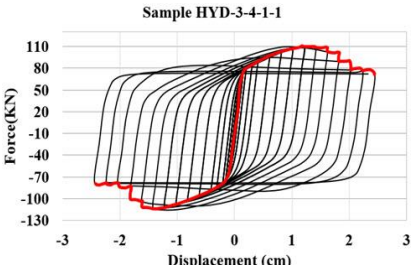

HYD-3-4-1-1

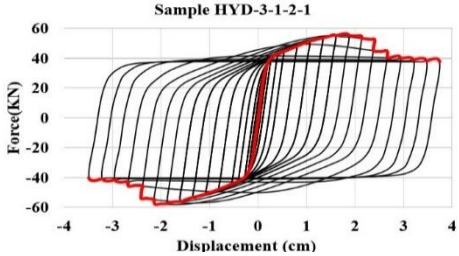

HYD-3-1-2-1

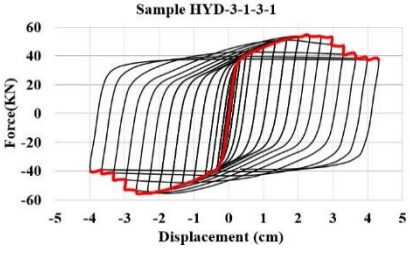

HYD-3-1-3-1

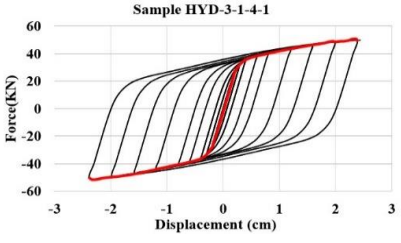

HYD-3-1-4-1

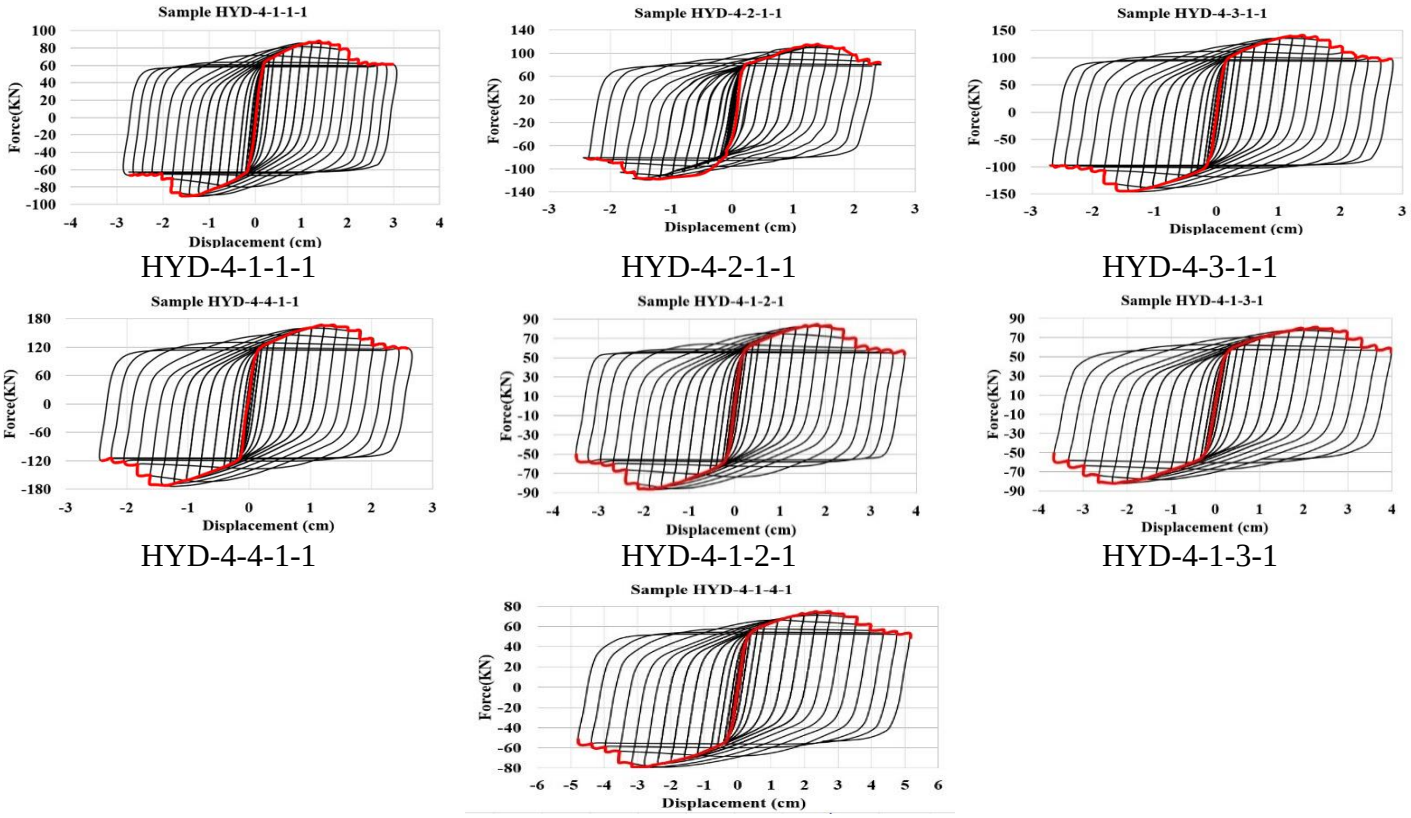

Fig. 12. Force-displacement hysteresis loops of the HYD and backbone curves

4. Mechanical parameters of DPMD dampers

4.1. Ductility ratio, effective and initial stiffness

Ductility ratio can be defined as the ratio of maximum deformation capacity to the deformation level corresponding to a yield deformation. The value of ductility ratio is given by:

$$\mu = \frac{\Delta_{max}}{\Delta_y} \quad (1)$$

Where Δ_{max} and Δ_y are ultimate displacement and yield displacement, respectively. In each loop of the force-deformation hysteresis curve the secant or effective stiffness can be defined. The effective stiffness for maximum displacement was obtained as the average from minimum and maximum force over the average from minimum and maximum displacement, respectively. According to Figure 13, effective stiffness equation is obtained as follows:

$$K_{eff} = \frac{\frac{|P_{max}|+|P_{min}|}{2}}{\frac{|\Delta_{max}+\Delta_{min}|}{2}} = \frac{P_{ave}}{\Delta_{ave}} \quad (2)$$

Where Δ_{max} , Δ_{min} , Δ_{ave} , P_{max} , P_{min} and P_{ave} are ultimate displacement, minimum displacement, average displacement, ultimate force, minimum force, average force in each loop, respectively. In this research, effective stiffness was calculated for maximum displacement and last loop of the force displacement hysteresis curves of the HYD samples. Also, initial stiffness is calculated as follows:

$$K_{initial} = \frac{P_y}{\Delta_y} \quad (3)$$

Where Δ_y and P_y are yield displacement and yield force, respectively. In this paper, initial stiffness was calculated for first loop of the force-

displacement hysteresis curves of the HYD samples. Effective stiffness represents the damping force in response to the desired displacement. The ultimate displacement and yield displacement values were obtained from the force-displacement hysteresis curve. Table 2 illustrates the ductility ratio, effective stiffness and initial stiffness for the HYD samples. Figure 13 shows the effective stiffness, dissipated energy, and elastic strain energy in the last loop of the hysteresis curve [19]. Figures 14 and 15 show the Ductility ratio (μ) and effective stiffness (K_{eff}) of HYD samples.

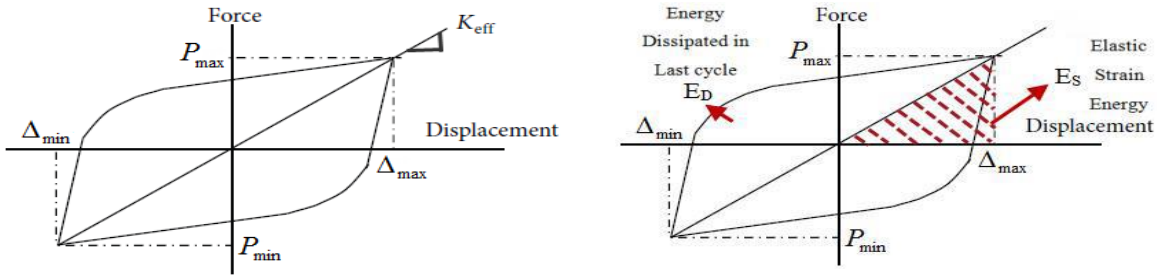

Fig. 13. Effective stiffness, dissipated energy and elastic strain energy in the last loop of the hysteresis curve [19]

Table 2. Ductility ratio, effective stiffness and initial stiffness of HYD samples

Number	Sample	Δ_y (cm)	Δ_{max} (cm)	Δ_{min} (cm)	Δ_{ave} (cm)	P_y (KN)	P_{min} (KN)	P_{max} (KN)	P_{ave} (KN)	μ	k_{inital} (KN/cm)	k_{eff} (KN/cm)
1	HYD-1-1-1-1	0.1186	1.232	-0.879	1.0561	19.01	-28.73	26.94	27.83	10.38	160.2	26.35
2	HYD-1-2-1-1	0.1388	1.214	-1.419	1.3164	22.80	-36.31	35.30	35.96	8.73	164.1	27.31
3	HYD-1-3-1-1	0.1751	1.201	-1.370	1.2862	30.12	-43.91	43.26	43.58	6.86	172.0	33.88
4	HYD-1-4-1-1	0.1872	1.431	-0.923	0.1775	36.36	-53.26	49.62	51.44	7.64	194.2	43.68
5	HYD-1-1-2-1	0.18	1.58	-1.83	1.70	17.12	-27.65	26.94	27	8.79	95.10	15.99
6	HYD-1-1-3-1	0.26	2.61	-2.44	2.52	17.26	-25.56	24.79	25	9.89	65.50	9.97
7	HYD-1-1-4-1	0.23	2.75	-2.74	2.74	14.76	-24.56	23.88	24	12.03	64.50	8.82
8	HYD-2-1-1-1	0.1331	1.395	-1.588	1.4915	27.91	-43.69	42.42	43.05	10.48	209.8	28.86
9	HYD-2-2-1-1	0.1147	1.201	-1.024	1.1128	33.07	-56.81	55	55.90	10.47	288.3	50.24
10	HYD-2-3-1-1	0.1388	1.407	-1.370	1.3888	45.82	-69.12	67.57	68.34	10.13	329.9	49.21
11	HYD-2-4-1-1	0.1388	1.201	-1.346	1.2741	54.24	-82.12	80.30	81.21	8.65	390.5	63.73
12	HYD-2-1-2-1	0.2184	1.582	-2.105	1.84	27.94	-42.48	40.93	42	7.24	127.9	22.62
13	HYD-2-1-3-1	0.2626	2.274	-2.551	2.41	26.42	-40.09	39.78	40	8.66	100.6	16.55
14	HYD-2-1-4-1	0.2226	2.318	-2.730	2.52	21.74	-39.00	37.44	38	10.41	97.60	15.12
15	HYD-3-1-1-1	0.1319	1.398	-1.607	1.5042	35.92	-60.13	58.76	59.45	10.06	272.2	39.52
16	HYD-3-2-1-1	0.1247	1.598	-1.385	1.4920	43.25	-77.62	74.66	76.14	12.82	456.2	51.03
17	HYD-3-3-1-1	0.1217	1.415	-1.430	1.4231	53.33	-96.29	94.07	95.18	11.62	437.9	66.88
18	HYD-3-4-1-1	0.1326	1.391	-1.087	1.239	69.33	-108.8	109.8	109.3	10.48	522.5	88.18
19	HYD-3-1-2-1	0.1959	1.834	-2.106	1.97	36.12	-58.45	56.38	57	9.36	145.3	20.41
20	HYD-3-1-3-1	0.2069	2.252	-2.614	2.43	32.10	-55.86	54.70	55	10.88	181.4	29.13
21	HYD-3-1-4-1	0.1965	2.362	-2.329	2.35	25.89	-51.47	50.69	51	12.02	131.8	21.77
22	HYD-4-1-1-1	0.1522	1.400	-1.415	1.4079	53.33	-90.37	88.14	89.25	9.2	350.3	63.39
23	HYD-4-2-1-1	0.1595	1.390	-1.359	1.3749	73.62	-118.2	115.1	116.6	8.71	461.5	84.85
24	HYD-4-3-1-1	0.1058	1.405	-1.359	1.3828	75.55	-144.4	141.1	142.8	13.28	713.8	103.2
25	HYD-4-4-1-1	0.094	1.385	-1.40	1.3931	97.33	-172	166.6	169.3	14.61	1026.	121.5
26	HYD-4-1-2-1	0.16	1.81	-1.89	1.85	50.90	-86.32	84.39	85	11.40	321.3	46.17
27	HYD-4-1-3-1	0.17	2.31	-2.29	2.30	42.72	-82.64	80.31	81	13.91	257.3	35.45
28	HYD-4-1-4-1	0.19	2.75	-3.15	2.95	39.52	-79.31	74.83	77	14.19	203.8	26.13

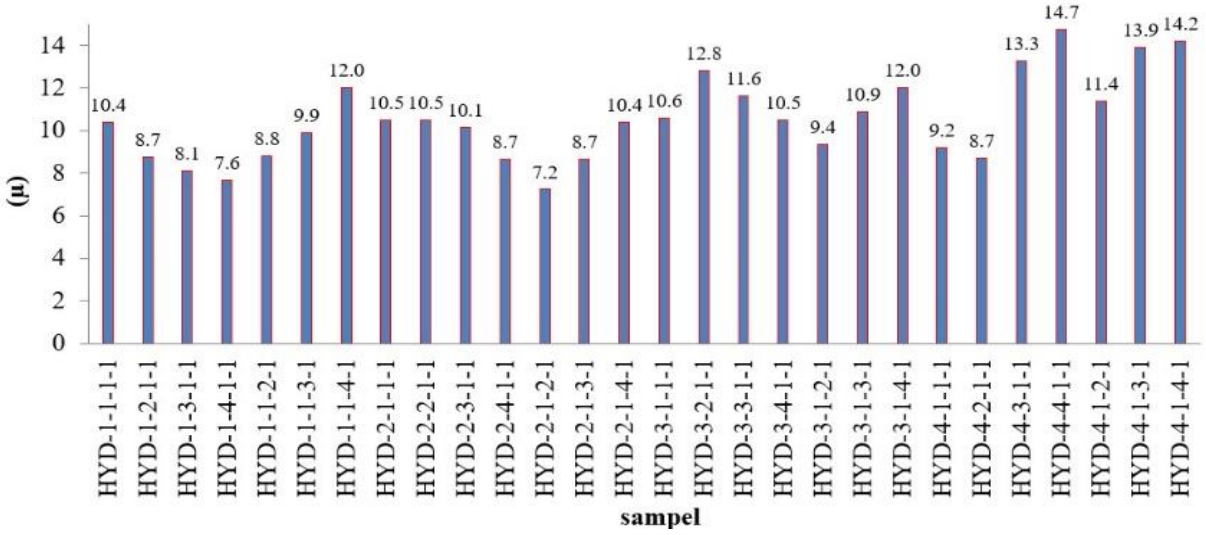

Fig. 14. Ductility ratio (μ) of HYD samples.

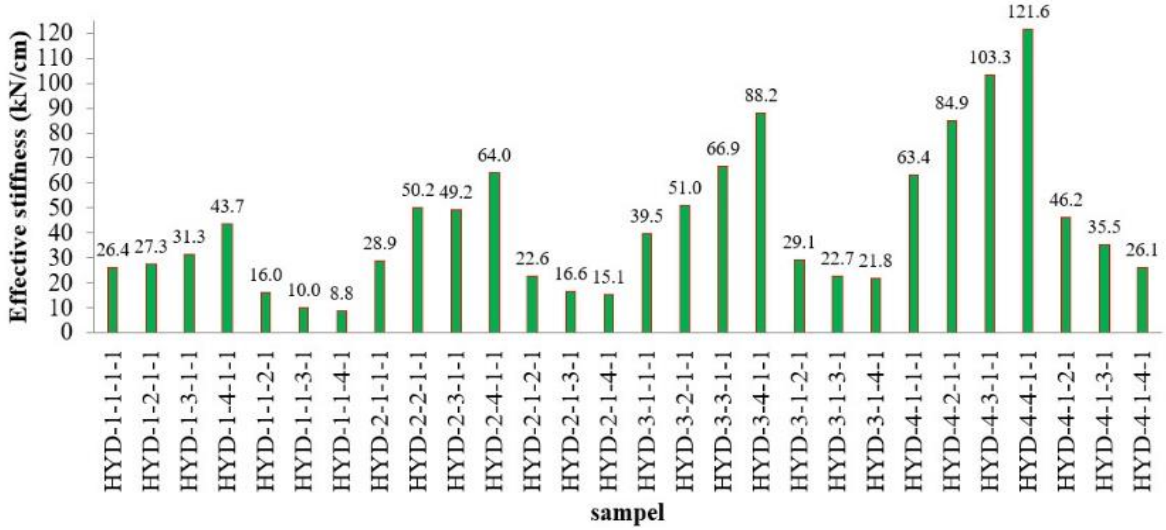

Fig. 15. effective stiffness (K_{eff}) of HYD samples.

According to Figure 14 by increasing the sample length from 41.80 cm to 75.28 cm, the Ductility ratio in HYD samples decreases and by increasing the height from 20.32 cm to 39.65 cm, this ratio increases. HYD-4-4-1-1 sample has the highest Ductility ratio, which is increased by 26.34% compared to HYD-1-1-1-1 sample. The lowest Ductility ratio is related to the HYD-2-1-2-1 sample, which is reduced by 35.64% compared to the HYD-1-1-1-1 sample. Also, due to the increase in the thickness of the samples, it can be expected that the amount of Ductility will increase.

According to the values obtained from Figure 15, with the increase in the length of the sample, the effective stiffness increases and with the increase in the height of the sample, the effective stiffness decreases. The effective stiffness of samples HYD-1-1-1-1 to HYD-1-4-1-1 increased by 49.47% with increasing length. Also, with the increase in height in samples HYD-1-1-2-1 to HYD-1-1-4-1, the effective stiffness value decreases by 57.79%. The highest value of effective stiffness corresponds to HYD-4-4-1-1sample, which is 121.57 KN/cm. The thickness of this sample is 1.44 cm and its maximum length is 75.28 cm. its effective stiffness has increased by

128.74% compared to HYD-1-1-1-1 sample. The lowest effective stiffness value among the HYD samples corresponds to the HYD-1-1-4-1 sample at the rate of 82.8 KN/cm, which has a thickness of 0.48 cm and a maximum height of 39.65 cm. Compared with HYD-1-1-1-1 sample, it is reduced by 99.68%.

4.2. Hysteresis damping coefficient

The equivalent viscous damping (EVD) or effective damping is effective index in evaluating the seismic performance of passive energy dissipation systems. The EVD has defined the combined effects of elastic and hysteretic damping. The EVD concept was first proposed by Jacobsen [17, 18]. The value of EVD based on Jacobsen's approach can be calculated with equation 4. The ξhyst represents the dissipation energy due to the hysteretic behavior.

$$\zeta_{hyst} = \frac{E_D}{4\pi E_S} = \frac{E_D}{2\pi K_{eff}\delta_{ave}^2} \quad (4)$$

Table 3 shows the value of ζhyst for 28 HYD samples for the ultimate displacement.

Table 3. Total dissipated energy (E_T), dissipated energy in the last cycle (E_D)elastic strain energy (E_S) and EVD of HYD samples and proposed formula

Number	Sample	E_T (KN.cm)	E_D (KN.cm)	E_S (KN.cm)	$\frac{E_D}{E_T}$	$\frac{E_S}{E_T}$	ζhyst (%)
1	HYD-1-1-1-1	1555.745	175.956	14.70	11.30%	0.90%	95.30
2	HYD-1-2-1-1	2170.369	241.565	23.70	11.10%	1.10%	81.20
3	HYD-1-3-1-1	2620.033	285.454	28	10.90%	1.10%	81.10
4	HYD-1-4-1-1	3275.423	347.831	30.30	10.60%	0.90%	91.40
5	HYD-1-1-2-1	2178.70	252.30	23.20	11.60%	1.10%	86.50
6	HYD-1-1-3-1	2182	266.90	31.80	12.20%	1.50%	66.90
7	HYD-1-1-4-1	1417.90	2160.80	33.20	15.30%	2.30%	51.90
8	HYD-2-1-1-1	1574.569	283.68	32.10	11.00%	1.20%	70.30
9	HYD-2-2-1-1	3313.167	363	31.10	11.00%	0.90%	92.90
10	HYD-2-3-1-1	4123.802	452.778	47.50	11.00%	1.20%	75.90
11	HYD-2-4-1-1	4884.673	536.30	51.50	11.00%	1.10%	82.80
12	HYD-2-1-2-1	2625.27	331.859	38.50	12.60%	1.50%	68.70
13	HYD-2-1-3-1	3994.18	443.737	48.20	11.10%	1.20%	73.30
14	HYD-2-1-4-1	3747.993	725.356	28.20	12.20%	1.30%	75.30
15	HYD-3-1-1-1	3792.095	420.487	44.70	11.10%	1.20%	74.80
16	HYD-3-2-1-1	6941.531	678.85	56.80	9.80%	0.80%	95.10
17	HYD-3-3-1-1	5642.711	634.05	67.70	11.20%	1.20%	74.50
18	HYD-3-4-1-1	5970.836	705.07	67.70	11.80%	1.10%	82.90
19	HYD-3-1-2-1	4505.663	531.433	56.60	11.80%	1.30%	74.80
20	HYD-3-1-3-1	4728.451	591.408	67.30	12.30%	1.40%	70.00
21	HYD-3-1-4-1	2053.467	296.276	59.90	14.40%	2.90%	39.30
22	HYD-4-1-1-1	6362.079	681.712	62.80	10.70%	1.00%	86.40
23	HYD-4-2-1-1	5247.384	706.925	80.20	13.50%	1.50%	70.10
24	HYD-4-3-1-1	9057.625	998.212	98.70	11.00%	1.10%	80.50
25	HYD-4-4-1-1	9557.765	1096.64	117.90	11.50%	1.20%	74.00
26	HYD-4-1-2-1	6659	763.50	78.90	11.50%	1.20%	77.00
27	HYD-4-1-3-1	6257	817	93.60	13.10%	1.50%	69.50
28	HYD-4-1-4-1	8064.90	992.80	113.60	12.30%	1.40%	69.50

According to table 3, the hysteresis damping of the sample HYD-1-1-1-1 with a thickness of 0.48 cm is 95.30%. Compared to the sample HYD-4-1-1-1 with a thickness of 1.44 cm, this amount has decreased by 86.40%. Therefore, with the increase in the thickness of the sample, the hysteresis damping decreases. Also, by increasing the height of the HYD-1-1-4-1 sample by 39.65 cm, the hysteresis damping decreases by 51.90% compared to the HYD-1-1-1-1 sample.

5. Conclusions

In this research, a new type of yielding metal dampers called honeycomb dampers was introduced. According to the analysis, it was found that the effective stiffness increases with the increase in the length of the sample. Also, as the height of the sample increases, the effective stiffness also decreases. As the sample thickness increases, the effective stiffness also increases.
The highest effective stiffness value is related to the HYD-4-4-1-1 sample, which has the longest length and the largest thickness, and its effective stiffness is equal to 121.57 kN/cm. Therefore, with the increase in the length and thickness of the sample, the effective stiffness value increased and with the increase of the height of the sample, the effective stiffness decreases. Also, the Ductility ratio decreases with increasing sample length and increases with increasing sample height. According to the values obtained from Table 3, it can be concluded that with the increase in the height of the HYD samples, the hysteresis or effective damping coefficient decreases and with the increase in the length and thickness of the HYD samples, the hysteresis damping coefficient increases slightly. In the end, it is suggested that the performance of the honeycomb yielding damper is improved by increasing the length and thickness.

6. References

[1]. Kelly J.M, Skinner R.1, Heine A.J. Mechanisms of Energy Absorption in Special Devices for Use in Earthquake Resistant Structures. Bulletin of N. Z. Society of Earthquake Engineering, Vol. 5 No. 3, 1972.

[2]. Skinner R.1, Kelly J.M, Heine A.J. Hysteretic Dampers for Earthquake Resistant Structures. Earthquake Engineering and Structural Dynamics, 287- 296, 1975.

[3]. Skinner R.1, Tyler R.G, Heine A.J, Robinson W.H. Hysteretic Dampers for the Protection of Structures from Earthquakes. Bulletin of N. Z. Society of Earthquake Engineering, Vol 13. No 1, 1980.

[4]. Kasai K, Popov E.P. General behavior of WF steel shear link beams. J. Struc. Eng, 112(2): 362-382, 1986.

[5]. Bergman D. M, Goel S.C. Evaluation of cyclic testing of steel plate device for added damping and stiffness. Report No. UMCE 87-10, the University of Michigan, Ann Arbor, MI, 1987.

[6]. Whittaker A.S, Bertero V.V, Thompson C. L, Alonso L.J. Seismic Testing of Steel Plate Energy Dissipation Devices. Earthquake Spectr; 7(4): 563-604, 1991.

[7]. Tsai K.C, Chen H.W, Hong C.P, Su Y.F. Design of steel triangular plate energy absorbers for seismic-resistance construction. Earthquake Spectra; 9(3): 505-528, 1993.

[8]. Dargush G.F, Soong T.T. Behavior of Metallic Plate Dampers in Seismic Passive Energy Dissipation Systems. Earthquake Spectra; 11(4): 545-568, 1995.

[9]. Gang Li, Hongnan Li. Earthquake resistant design of RC frame with dual functions metallic damper. The 14th World Conference on Earthquake Engineering. Beijing, China, 2008.

[10]. Soni A.H, Sanghvi C.S. Mathematical modeling of ADAS damper element and nonlinear time history analysis of SDOF steel structure using ETABS. Journal of Engineering Research and Studies, 2012.

[11]. Teruna D.R, Majid T.A, Budiono B. Experimental Study of Hysteretic Steel Damper for Energy Dissipation Capacity. Advances in Civil Engineering, Article ID 631726, 12 pages, 2015.

[12]. Sahoo D.R, Singhal T, Taraithia S.S, Saini A. Cyclic behavior of shear-and-flexural yielding metallic dampers. Journal of Constructional Steel Research; (114): 247–257, 2015.

[13]. Garivani S, Aghakouchak A.A, Shahbeyk S. Numerical and Experimental Study of Comb-Teeth Metallic Yielding Dampers. International Journal of Steel Structures; 16(1): 177-196, 2016.

[14]. Ghaedi K, Ibrahim Z, javanmardi A. A new metallic bar damper device for seismic energy dissipation of civil structures. 14th International Conference on Concrete Engineering and Technology, 2018.

[15]. Kiai, M. Evaluation of the performance of metal yielding dampers in steel structures, Faculty of Civil Engineering, Noshirvan University of Technology, Babol, 2018.

[16]. Moghadasi M, Namazi A. Assessment of pearformance of TADAS dampers for the Seismic rehabilitation of buildings. International Journal of Applied Engineering Research; 11(21): 10516-10523, 2016.

[17]. Yang T.Y, Tianyi Li, Tobber L, Pan X. Experimental Test of Novel Honeycomb Structural Fuse. The 14th Nordic Steel Construction Conference, Copenhagen, Denmark, 451-456, 2019.

[18]. Yang T.Y, Banjuradja W, Tobber L. Experimental Test of Welded Wide Flange Fuses. key Engineering Materials; (763): 414-422, 2018.

[19]. Shadman Heidari P. numerical study on mechanical parameters of novel drilled plate metallic damper (DPMD). Proceedings of the 2nd Croatian Conference on Earthquake Engineering, 505-516, 2023.

[20]. ANSI/AISC 341-16. Seismic provisions for structural steel buldings. An american national standard, 9.1-148, 2016.

[21]. ANSYS Meshing User's Guide, (2016), Release 16.0. ANSYS, Inc.

[22]. Jacobsen L.S. Steady forced vibration as influenced by damping. Transactions of ASME, 52, 169-181, 1930.

[23]. Jacobsen L.S. Damping in composite structures, Proceedings of the Second World Conference on Earthquake Engineering, Vol 2, 1029-1044, (1960).